

Experimental study of the neck formation in an X pinch

A P Artyomov^{*}, S A Chaikovsky, A V Fedunin, N A Labetskaya, A G Rousskikh, A S Zhigalin, and V I Oreshkin

Institute of High Current Electronics SB RAS, 2/3 Akademicheskoy Ave., Tomsk, 634033, Russia

E-mail: aap545@gmail.com

Abstract. X-pinch experiments have been performed on a compact 250 kA, 180 ns pulsed power generator specially designed for this purpose at the Institute of High Current Electronics (Tomsk, Russia). The X pinches were composed of two molybdenum wires of diameter 25 μm making an angle of 36° with the z -axis. The X-pinch dynamics was recorded with a 3 ns exposure time using an HSFC Pro four-frame camera. Axial plasma jets propagating toward both the anode and the cathode were observed. The jets became noticeable within 10 ns after the onset of current flow, which approximately corresponded to the time at which the electrical explosion of the X-pinch wires occurred. The velocity of the anode-directed jet reached 10^7 cm/s, which was about 1.5 times the velocity of the cathode-directed jet. These high jet velocities are inconsistent with the plasma temperature resulting from the wire explosion. Hence, these jets seem to develop due to implosion of the light plasma layer stripped by magnetic forces from the wire surface, and the increase in their velocities is perhaps due to cumulative effects taking place at the X-pinch axis. The X-pinch neck formed as a rule above the initial wire cross point (closer to the anode). In this region, the plasma diameter gradually increased with time and then drastically decreased 10–15 ns prior to the x-ray pulse. Immediately before the x-ray pulse, in the (250–300 μm long) plasma neck, a lower scale constriction developed, forming a “hot spot”. It has been confirmed that the anode-directed plasma jet could take some part of the X-pinch wire current because of the evident jet pinching in the anode region. This process seems to determine the neck length.

1. Introduction

Two or more metal wires 10–50 μm in diameter crossed like the letter “X” are used as the so-called X-pinch loads for pulsed power generators. When a current pulse is passed through an X pinch, a plasma hot spot several micrometers in size can be produced. The hot spot efficiently radiates soft x-rays in a 1–2 ns pulse. Hot spots of this type are currently one of the brightest soft x-ray laboratory sources. The parameters of the X-pinch-based soft x-ray sources make them attractive for projection radiography of various short-living physical objects. Although X-pinches have been studied for long, since 1982 [1], they remain an object of intense fundamental research because of a number of interesting physical features. The emission properties of hot plasmas at near-solid densities, the radiative collapse, and the formation of supersonic jets are of most interest.

The sequence of physical processes leading to the formation of a hot spot can be revealed using a nanosecond time resolved diagnostics. Relevant experiments were carried out on different pulse generators using optical and x-ray frame imaging, interferometry imaging, and soft x-ray backlighting [2–11]. Nevertheless, the results obtained could not be properly interpreted because of strong



sensitivity of the X-pinch dynamics to the current pulse waveform. Since 2006, X-pinch experiments using a set of self-made compact pulsed power generators have been performed at the Institute of High Current Electronics (Tomsk, Russia). This paper presents the results of experiments aimed at studying the dynamics of X-pinch necking from the wire explosion stage to the formation of a hot spot.

2. Experimental setup

The experiments were carried out on a compact, 250-kA, 180-ns pulse generator specially designed for X-pinch studies [12–16]. The generator consists of four self-made 250-nF capacitors connected in parallel. Each capacitor is equipped with a built-in triggered gas switch. The X pinches were composed of two 25- μm molybdenum wires each making an angle of 36° with the z-axis.

The X-pinch dynamics was recorded with a 3-ns exposure time using an HSFC Pro four-frame camera. The frame interval was varied in the range 20–40 ns. Figure 1 shows a set of typical frames.

Horizontal lines indicate the initial position of the wire cross point, which is indicated by X_0 . The cathode position is at the bottom of each image. The fourth frame in Fig. 1 corresponds to the time of occurrence of an x-ray pulse.

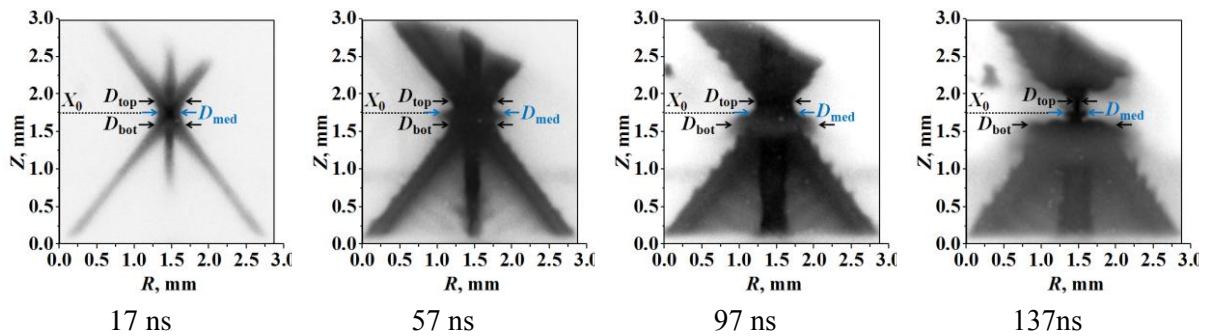


Figure 1. Typical optical pictures of an X pinch made of two 25- μm molybdenum wires taken in one shot: X_0 indicates the initial position of the wire cross point.

The X-pinch current was measured using a Rogowski coil. The x-ray emission was detected with a copper-cathode x-ray diode (XRD) filtered to view the spectral region $h\nu > 1$ keV. Figure 2 presents typical current and XRD signal traces. In all experimental shots, the time of x-ray pulse generation, $t_{x\text{-ray}}$, measured from the onset of current flow was 140 ± 5 ns.

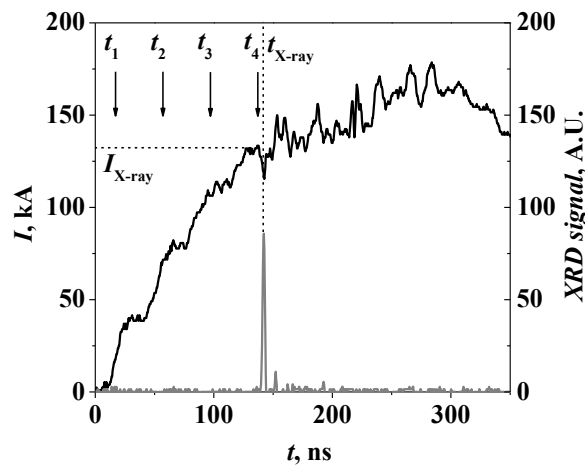


Figure 2. Typical current and XRD signal traces

The small spread in the time of x-ray pulse generation allowed us to compare X-pinch images taken in different shots. To do this, all pictures captured with different camera delays were combined to form

an integrated sequence of frames which would cover all stages of the X-pinch dynamics from the wire explosion to the disruption of the plasma neck. This integrated picture was used to determine the evolution of the diameter of an individual wire, the velocities of the axial plasma jets, and the plasma expansion/implosion velocity near the wire cross point.

3. X-pinch wire expansion and axial jet formation

The integrated sequence of frames captured in several shots is presented in Fig. 3. Each image is marked by relative time $t/t_{x\text{-ray}}$ ($t_{x\text{-ray}} = 140$ ns).

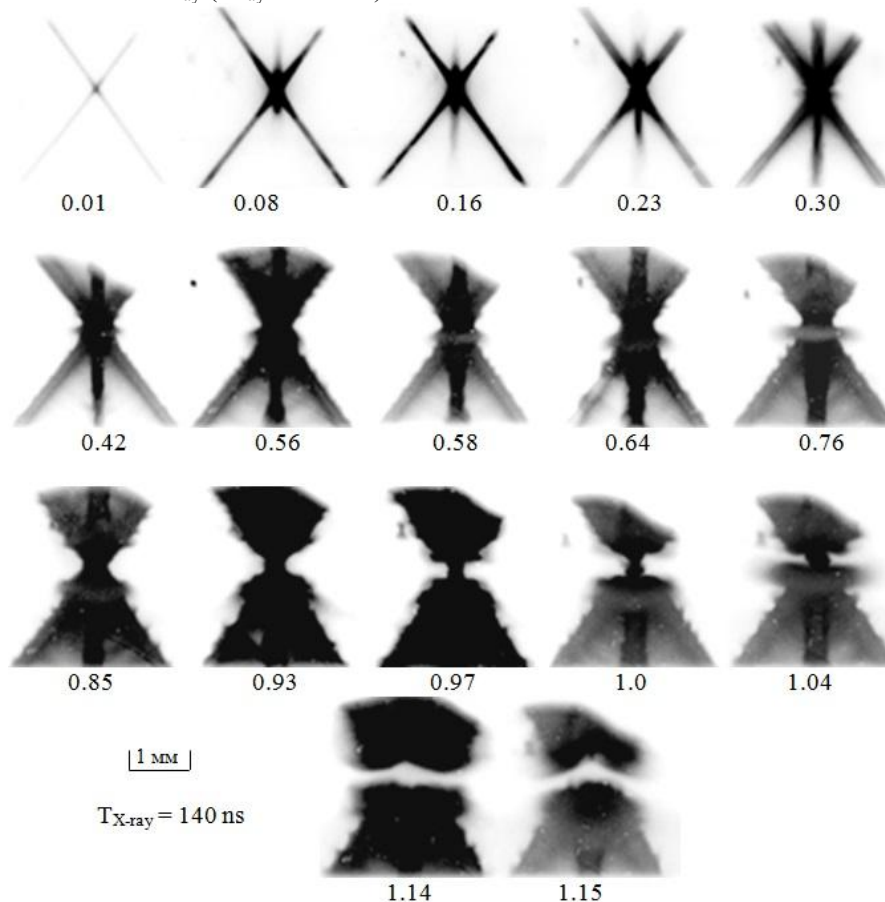


Figure 3. Integrated sequence of frames captured in several shots. The relative time $t/t_{x\text{-ray}}$ is given beneath each image.

At the initial stage of X-pinch dynamics, the wires explode and expand. Figure 4a shows the time variation of the distances R_{in} and R_{out} from the initial position of the axis of an individual wire to the expanding plasma edge, measured, respectively, toward and outward the other wire. If a wire would expand uniformly from its axis, the values of R_{in} and R_{out} should be equal and could be considered to be the wire radius. As can be seen in Fig. 4, the wire plasma expands symmetrically about the wire axis until the relative time $t/t_{x\text{-ray}} \approx 0.4$ ($t_{x\text{-ray}} = 140$ ns). The expansion velocity, slightly varying with time, is $(2.6\text{--}3.0) \cdot 10^5$ cm/s. The subsequent behavior of the wire plasma features a slightly rising inward velocity and full cessation of the outward expansion.

The wire radius increases about fourfold within the first 10 ns of the process due to thermal expansion of the surface plasma (see Fig. 4a). Clearly seen axial plasma jets propagating toward both the cathode and the anode are observed as early as within 2 ns. The velocity of the anode-directed jet, V_{top} , reaches $\sim 10^7$ cm/s, which is about 1.5 times the velocity of the cathode-directed jet (see Fig. 4b). These high jet velocities are inconsistent with the plasma temperature resulting from the wire explosion. Hence, these jets seem to develop due to implosion of the light plasma layer stripped by

magnetic forces from the wire surface, and the increase in their velocities is perhaps due to cumulative effects taking place at the X-pinch axis.

The X-pinch wires become nonuniform in structure at $t/t_{x\text{-ray}} \approx 0.3$. A highly luminous plasma corona is observed which surrounds a wire core whose brightness is considerably lower. The core diameter is approximately half that of the coronal plasma.

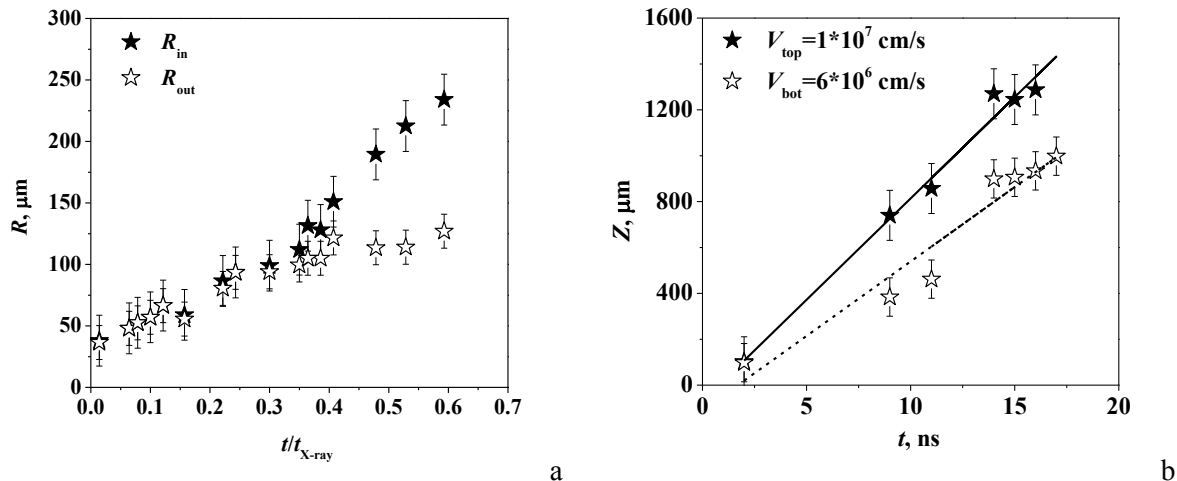


Figure 4. Time variation of R_{in} and R_{out} (a) and the axial plasma jet lengths measured from the wire cross point toward the anode (bold asterisks) and toward the cathode (open asterisks) (b): $t_{x\text{-ray}} = 140$ ns.

4. X-pinch necking

The main features of the X-pinch dynamics can be inferred from Fig. 3. At the initial stage ($t/t_{x\text{-ray}} < 0.16$), the plasma surrounding the cross point slightly expands, remaining shaped like a cone. A few nanoseconds later, a visible sausage-like perturbation develops near the cross point, and this is just the onset of neck formation. Along with the occurrence of the neck, a clearly visible plasma plume (or a radially expanding jet) is observed a little bit below the point X_0 . This plasma plume and the plasma located below the cross point show no evidence of implosion. Thus, the implosion occurs in the region that extends to about 500 μm above and including the cross point.

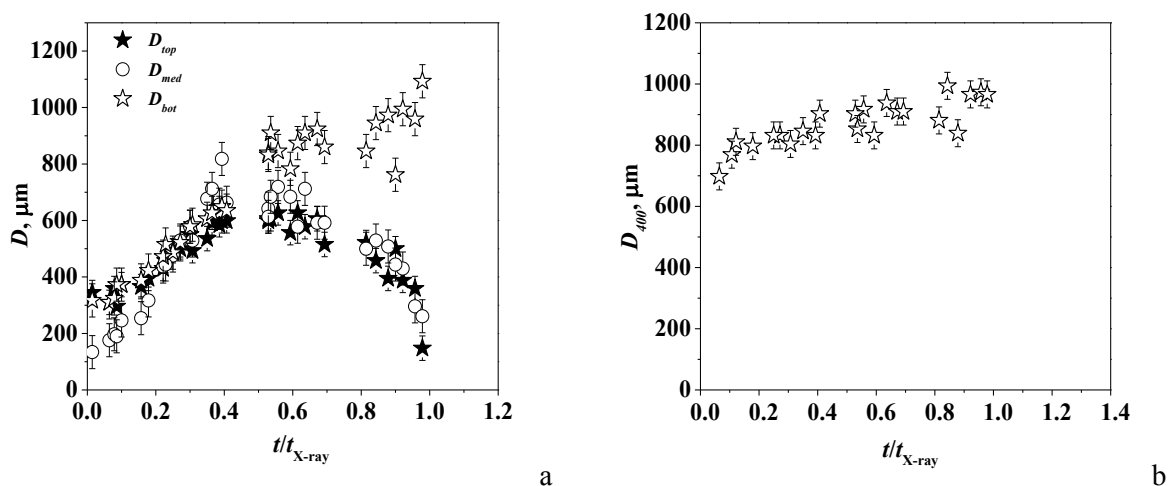


Figure 5. Plasma size measured in the horizontal cross-sections at the point X_0 (D_{med}), 150 μm above (D_{top}) and 150 μm below the point X_0 (D_{bot}) (a), and 400 μm above the point X_0 (D_{400}) (b). Immediately before the X-ray pulse is generated ($t/t_{x\text{-ray}} = 0.97$), a visible plasma pinch of length 200-300 μm is formed in which a constriction of significantly smaller size can be seen. This constriction

forms the X-pinch micrometer-size “hot spot”. The hot spot formation takes only a few nanoseconds or less.

The hot spot is located closer to the anode, 50–150 μm above the point X_0 . In this region, the plasma diameter gradually increases with time, showing an abrupt decrease 10–15 ns before the X-ray pulse (see Fig. 5a). Figure 5a presents the plasma size measured in the horizontal cross-sections at the point X_0 (D_{med}), 150 μm above (D_{top}) and 150 μm below the point X_0 (D_{bot}) (see Fig. 1). The plasma expansion in the neck region goes with a velocity of $3 \cdot 10^5$ cm/s until $t/t_{\text{x-ray}} \approx 0.4$, proceeding in fact in step with the expansion of an individual wire. The plasma expansion velocity at the point X_0 (see the data for D_{med} in Fig. 5a) is about half that in the case of purely radial jet formation (see Fig. 3, $t/t_{\text{x-ray}} = 0.3$).

A few nanoseconds later, the size D_{med} abruptly decreases. The reason is that the jet position is shifted downward, giving rise to the mentioned plasma plume on the cathode side. Subsequently, a pronounced implosion is observed in the region between the point X_0 (D_{med}) and the point located 150 μm above (D_{top}). The implosion velocity reaches $(3\text{--}5) \cdot 10^6$ cm/s at a radius of 100 μm .

It can be seen that the bottom part of the plasma (D_{bot} in size) does not implode. This is just the region of the plasma plume. The X-pinch plasma in the region 400 μm above the cross point also does not implode (see Fig. 5b). This seems to be due to the current switching to the axial plasma jet whose diameter is 400–600 μm . The switching can reduce the current flowing through the wires and slow down the implosion of the wires at a diameter greater than the jet diameter, resulting in a shorter neck.

The supposition that the current could partially flow through the axial jets is additionally supported by the observed implosion (pinching) of the top axial jet. This can clearly be seen in Fig. 6a. This image was taken for another X pinch made of four Mo wires of diameter 25 μm . Pinching of the near-anode (top) part of the axial plasma jet is evident.

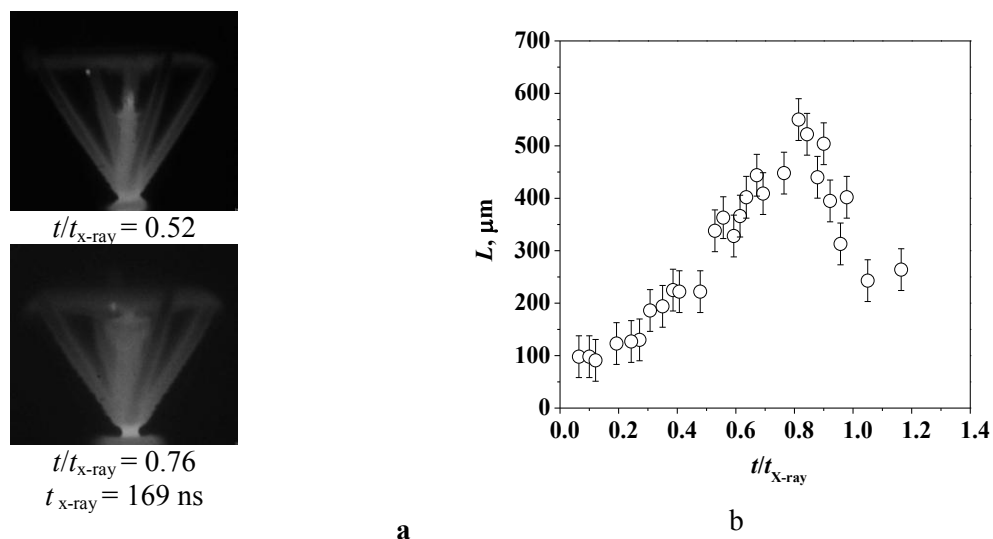


Figure 6. Typical optical images of an X pinch made of four molybdenum wires of diameter 25 μm , taken above the wire cross point (a) and the time variation of the neck length (L) in the cross-point region (b).

Figure 6b presents the measurements of the neck axial dimension, which could also be termed the neck length. It can be seen that neck length L strongly depends on time, increasing from 100 to 550 μm within 110 ns. Thereafter, the axial dimension of the perturbation decreases during 30 ns and becomes equal to 250–300 μm nearly at the time the x-ray pulse is generated. The increase of the neck length can be accounted for by the action of the axial component of the $\mathbf{J} \times \mathbf{B}$ force. The subsequent elongation of the neck can be accounted for by the progressive loss of linear mass in the middle of the neck due to the axial plasma outflow.

5. Conclusion

X-pinch experiments have been performed on a compact 250 kA, 180 ns pulse generator specially designed for this purpose at the Institute of High Current Electronics (Tomsk, Russia). The X pinches were composed of two molybdenum wires of diameter 25 μm making an angle of 36° with the z -axis. The X-pinch dynamics was recorded with a 3-ns exposure time using an HSFC Pro four-frame camera. Axial plasma jets propagating toward both the anode and the cathode were observed. The jets became noticeable within 10 ns from the onset of current flow, which approximately corresponded to the time at which the electrical explosion of the X-pinch wires occurred. The velocity of the anode-directed jet reached 10^7 cm/s, which was about 1.5 times the velocity of the cathode-directed jet. These high jet velocities are inconsistent with the plasma temperature resulting from the wire explosion. Hence, these jets seem to develop due to implosion of the light plasma layer stripped by magnetic forces from the wire surface, and the increase in their velocities is perhaps due to cumulative effects taking place at the X-pinch axis.

The X-pinch neck formed as a rule above the initial wire cross point (closer to the anode). In this region, the plasma diameter gradually increased with time and then drastically decreased 10–15 ns prior to the X-ray pulse. Immediately before the X-ray pulse, in the (250–300 μm long) plasma neck, a lower scale constriction developed, forming a “hot spot”. It has been confirmed that the anode-directed plasma jet could take some part of the X-pinch wire current because of the jet pinching in the anode region. This process seems to determine the neck length. We believe that the results obtained can be useful in theoretically modeling the X-pinch dynamics.

Acknowledgments

This work was supported in part by Presidium of the Russian Academy of Sciences under a program of “Fundamental Problems of Pulsed Power” and by the Russian Foundation for Basic Research (grant No. 12-08-00868-a).

References

- [1] Zakharov S M, Ivanenkov G V, Kolomenskii A A *et al.* 1982 *Sov. Tech. Phys. Lett.* **8** 456
- [2] Kalantar D H, Hammer D A, Dangor A E, Bayley J M and Beg F N 1994 *Citation: AIP Conf. Proc.* **299** 604
- [3] Choi P, Christou C and Aliaga R 1991 *SPIE* **1552** 270
- [4] Mitchell I H, Aliaga-Rossel R, Saavedra R, Chuaqui H, Favre M and Wyndham E S 2000 *Phys. Plasmas* **7** 5140
- [5] Pikuz S A, Shelkovenko T A, Sinars D B *et al.* 2001 *J. Quant. Spectr. Radiat. Trans.* **71** 581
- [6] Shelkovenko T A, Sinars D B, Pikuz S A and Hammer D A 2001 *Phys. Plasmas* **8** 1305
- [7] Green J S, Bland S N, Collett M, Dangor A E, Krushelnick K, Beg F N and Ross I 2006 *Appl. Phys. Lett.* **88** 261501
- [8] Beg F N, Ciardi A, Ross I, Zhu Y, Dangor A E and Krushelnick K 2006 *IEEE Trans. Plasma Sci.* **34** 2325
- [9] Chittenden J P, Ciardi A, Jennings C A, Lebedev S V, Hammer D A, Pikuz S A and Shelkovenko T A 2007 *Phys. Rev. Lett.* **98** 025003
- [10] Madden R E, Bott S C, Haas D, Eshaq Y, Ueda U, Collins G and Beg F N 2008 *Phys. Plasmas* **15** 112701
- [11] Collins G W, Valdivia M P, Zick T, Madden R E, Haines M G and Beg F N 2013 *Phys. Plasmas* **20** 042704
- [12] Artyomov A P, Fedyunin A V, Chaikovskiy S A, Zhigalin A S, Oreshkin V I, Ratakhin N A and Rousskikh A G 2013 *Instrum. Exp. Tech.* **56** 66
- [13] Ratakhin N A, Fedushchak V F, Erfort A A *et al.* 2007 *Izv. Vyssh. Uchebn. Zaved., Fiz.* **50** 87
- [14] Artemov A, Labetskaya N, Fedyunin A and Chaikovskii S 2010 *Bull. Leb. Phys. Inst.* **37** 31
- [15] Rousskikh A G, Oreshkin V I, Chaikovskiy S A *et al.* 2008 *Phys. Plasmas* **15** 102706
- [16] Mesyats G A, Shelkovenko T A, Ivanenkov G V *et al.* 2010 *Russ. Phys. JETP* **111** 363